Atmos. Chem. Phys. Discuss., 14, 31409–31440, 2014
www.atmos-chem-phys-discuss.net/14/31409/2014/
doi:10.5194/acpd-14-31409-2014


Atmospheric Chemistry and Physics Discussions



# Role of updrafts in aerosol-cloud interactions: lidar observations of layered warm clouds over central Europe

**J. Schmidt, A. Ansmann, J. Bühl, and U. Wandinger**

Leibniz Institute for Tropospheric Research, Leipzig, Germany

Received: 18 November 2014 – Accepted: 24 November 2014
– Published: 12 December 2014

Correspondence to: A. Ansmann (albert@tropos.de)

Published by Copernicus Publications on behalf of the European Geosciences Union.







## Abstract

Twenty nine cases of layered liquid-water cloud systems were observed with dual-field-of-view (dual-FOV) Raman lidar over the polluted central European site of Leipzig, Germany, between September 2010 and September 2012. For the first time, a detailed lidar-based study of aerosol-cloud-dynamics relationship was conducted. A collocated Doppler lidar provided information on vertical velocity and thus on updraft and downdraft occurrence. The novel dual-FOV lidar permits the retrieval of the particle extinction coefficient (used as aerosol proxy just below cloud base) and cloud properties such as droplet effective radius and cloud droplet number concentration in the lower part of optically thin cloud layers. Here, we present the key results of our statistical analysis of the 2010–2012 observations. Besides a clear aerosol effect on cloud droplet number concentration in the lower part of the convectively weak cloud layers during updraft periods, meteorological effects (turbulent mixing, entrainment of dry air) were found to diminish the observable aerosol effect higher up in the clouds. The corresponding aerosol-cloud interaction (ACI) parameter based on changes in cloud droplet number concentration with aerosol loading was found to be close to 0.8 at 30–70 m above cloud base during updraft periods which points to values around 1 at cloud base (0–30 m above cloud base). Our findings are extensively compared with literature values and agree well with airborne observations. As a conclusion, ACI studies over continental sites should include vertical wind observations to avoid a bias (too low values) in the obtained ACI results.

## 1 Introduction

The indirect aerosol effect on climate results from two cloud-influencing aspects. Atmospheric aerosol particles act as cloud condensation nuclei (CCN) in liquid-water droplet formation and as ice nuclei (IN) in processes of heterogeneous ice nucleation. The same CCN may serve, later on after lifting and cooling of the cloud parcel, as IN





ACPD
14, 31409–31440, 2014



via the immersion freezing process. There is no doubt that aerosols play a key role in the evolution of warm (pure liquid-water) and mixed-phase clouds and in the formation of precipitation and that anthropogenic and natural aerosols thus sensitively influence the atmospheric water cycle as a whole. Aerosol-cloud interaction (ACI) at given meteorological conditions must be well understood and properly parameterized in atmospheric circulation models to improve future climate predictions. The models must be able to handle all natural and man-made aerosol types from the emission over regional and long-range transport to deposition and the interaction of the different aerosols with the radiation field of the Earth's atmosphere and clouds. However, we are far away from a good representation of aerosols and their complex role in the climate system in computer models, especially with respect to aerosol vertical layering so that the uncertainties in climate predictions remain very high.

We need strong efforts of continuous, long-term observations of aerosols and clouds around the globe by means of active remote sensing (cloud radar, aerosol/cloud lidar) in the framework of well-coordinated ground-based networks and, complementary, also from space to overcome this unsatisfactory situation. CLOUDNET (Illingworth et al., 2007) may be regarded as a prototype network for the development of ground-based aerosol and cloud monitoring infrastructures. Continuous detection of all aerosol layers and embedded warm, mixed-phase, and ice clouds with high vertical and temporal resolution is required. In addition, measurements of vertical movements (updrafts, downdrafts, gravity waves) are demanded because vertical motions control all cloud processes (Twomey, 1959; Ghan et al., 1993, 1997, 2011; Morales and Nenes, 2010). New techniques as well as new combinations of existing techniques and tools need to be introduced to improve our ability to study ACI in the necessary detail and to provide in this way fundamental, reliable information for the improvement of cloud parameterization schemes in cloud-resolving models.

Recently, Schmidt et al. (2013, 2014b) presented a new lidar technique for warm-cloud ACI studies. The novel dual-field-of-view (dual-FOV) Raman lidar allows us to measure aerosol particle extinction coefficients (used as aerosol proxy) close to cloud





ACPD
14, 31409–31440, 2014



base and to retrieve cloud microphysical properties such as cloud droplet effective radius $r_e$ and cloud droplet number concentration (CDNC) in the lower part of the cloud. The development of this novel lidar technique was motivated by numerous published ACI studies (see Sect. 4), in which aerosol observations (at ground or far below cloud base) were correlated with remote-sensing products in terms of cloud-column-averaged effective radius or cloud mean droplet number concentration to describe the impact of a given aerosol load on the evolution and microphysical properties of a cloud layer. To our opinion, such experimental approaches do not allow an accurate quantification of ACI. We will discuss this issue in detail in Sect. 4.

Schmidt et al. (2014a) used this new dual-FOV Raman in combination with a co-located Doppler lidar to simultaneously monitor aerosol and cloud properties together with the vertical-wind field. This is a favorable remote-sensing approach for warm-cloud ACI studies because it allows us to investigate the direct impact of aerosol particles on cloud droplet nucleation as well as the role of up and downdrafts in warm-cloud ACI processes, and thus to obtain an improved insight into aerosol-related and dynamics-related aspects of warm-cloud processes. Furthermore, the role of entrainment and downward mixing of air to damp an aerosol signature on cloud microphysical properties can be investigated. Alternative approaches to Doppler lidar observations of vertical motions are cloud radar measurements. However, cloud radar observations of vertical motions are frequently biased by a few large falling drizzle droplets as our three-year experience with simultaneous Doppler lidar and Doppler radar observations shows.

Schmidt et al. (2014a) presented several case studies of combined dual-FOV Raman lidar and Doppler lidar observations of optically thin liquid-water altocumulus clouds. Key findings of exemplary lidar observations of layered clouds occurring over the polluted continental European site of Leipzig, Germany, in the lower free troposphere between 2.5 and 4 km height were discussed. Cases with clouds in clean and polluted aerosol environments were contrasted.

In this paper, we summarize our multi-year observations. We present the main results of a statistical analysis of 29 cloud cases observed from September 2010 to





ACPD
14, 31409–31440, 2014



September 2012. Lidar profiling through water clouds from bottom to top is only possible up to cloud optical depths of 3.0 and respective liquid water paths (LWPs) of up to about 50 g m$^{-2}$. Our statistics thus covers thin altocumulus clouds only. Nevertheless, the message of the paper is clear: only during updraft periods an unambiguous and strong relationship between aerosol burden and cloud microphysical properties is observed. This is the main topic of the paper and will be discussed in Sect. 3.

We begin with a brief description of the remote sensing instrumentation in Sect 2. Definitions of well-established aerosol-cloud interaction parameters are given in the Sect. 2, too. Section 3 discusses the experimental findings in terms of ACI statistics, and Sect. 4 provides an extended comparison of ACI literature values. A summary and concluding remarks are given in Sect. 5.

## 2 Lidar instrumentation and ACI parameters

The dual-FOV Raman lidar is described in Schmidt et al. (2013, 2014a, b). It permits us to characterize warm clouds (no ice phase) in terms of height profiles of single-scattering droplet extinction coefficient $\alpha$, cloud droplet number concentration $N$ (or CDNC), droplet effective radius $r_e$, and liquid water content LWC. The new technique is implemented in a multiwavelength polarization/Raman lidar so that detailed information of aerosol properties below cloud base are available in addition. We use the aerosol particle extinction coefficient $\alpha_p$ measured at 532 nm as aerosol proxy. Details on vertical and temporal resolution of the measurements and the uncertainties in the products can be found in Schmidt et al. (2014a).

The Doppler lidar provides vertical-wind information at cloud base and within optically thin cloud layers with vertical resolution of 70 m and a temporal resolution of a few seconds (Ansmann et al., 2009, 2010). The lidar was originally developed for vertical aerosol flux observations in the boundary layer (Engelmann et al., 2008).

Both lidars belong to the Leipzig Aerosol and Cloud Remote Observation System (LACROS, 51.3° N, 12.4° E) (Wandinger et al., 2012; Bühl et al., 2013) of the Leibniz





ACPD
14, 31409–31440, 2014



Institute for Tropospheric Research (TROPOS), Leipzig, Germany. Besides the lidars, further cornerstones of LACROS are a 35 GHz cloud radar and a microwave radiometer (MWR) for the determination of the liquid water path (LWP), which can be compared with the column-integrated liquid water content, LWC, obtained from the dual-FOV Raman lidar observations. LACROS belongs to the European Aerosol Research Lidar Network (EARLINET) and to the CLOUDNET consortium. Leipzig is also an Aerosol Robotic Network (AERONET) station.

To better quantify the aerosol effect on cloud properties (in Sect. 3) and to better compare our results with literature values (in Sect. 4), we computed two well-established ACI parameters (Feingold et al., 2001; Garrett et al., 2004; McComiskey and Feingold, 2008; McComiskey et al., 2009).

The nucleation-efficiency parameter is defined as:

$$\mathrm{ACI_N} = \mathrm{d}\ln(N)/\mathrm{d}\ln(\alpha_\mathrm{p}) \quad (1)$$

with the cloud droplet number concentration $N$ and the aerosol particle extinction coefficient $\alpha_\mathrm{p}$. $\mathrm{ACI_N}$ describes the relative change of the droplet number concentration with a relative change in the aerosol loading.

The indirect-effect parameter $\mathrm{ACI_r}$ is defined as:

$$\mathrm{ACI_r} = -\partial\ln(r_\mathrm{e})/\partial\ln(\alpha_\mathrm{p})\,. \quad (2)$$

$\mathrm{ACI_r}$ describes the relative change of the droplet effective radius $r_\mathrm{e}$ with a relative change in the aerosol extinction coefficient $\alpha_\mathrm{p}$ at constant LWP (or LWC) conditions. $\mathrm{ACI_r}$ is equal to 1/3 $\mathrm{ACI_N}$ (for constant LWP) according to the $r_\mathrm{e} \propto N^{-1/3}$ relationship. More details can be found in Schmidt et al. (2014a).





ACPD
14, 31409–31440, 2014



## 3 Statistical analysis

### 3.1 Overview of aerosol and cloud properties

29 dual-FOV Raman lidar cloud measurements are available for statistical analyses. These measurements were performed during nighttime between September 2010 and September 2012. All investigated clouds were geometrically and optically thin pure-liquid water clouds. Table 1 summarized the main aerosol and cloud properties of the 29 aerosol/cloud cases. The derived 532 nm aerosol particle extinction coefficients below cloud base ranged from 7–130 $Mm^{-1}$ with a mean value of $52 \pm 34$ $Mm^{-1}$. These aerosol conditions matches well with findings of Mattis et al. (2004) who presented aerosol lidar results for the boundary layer and lower free troposphere over the EARLINET station at Leipzig between 2000 and 2003. Base heights and vertical extend of the observed cloud layers ranged from about 1–4.5 km and 100–300 m, respectively. Table 2 summaries the cloud products derived from the dual-FOV Raman lidar observations. Most effective cloud droplet radii were found in the range from 5–10 µm and CDNCs showed typical values from 50–200 $cm^{-3}$.

### 3.2 Lidar-derived $ACI_r$ vs. $ACI_N$

Figure 1 illustrates how we tried to link aerosol properties with cloud properties. As aerosol proxy we used the particle extinction coefficient $\alpha_p$ for the layer from 300–1000 m below cloud base. These 532 nm extinction coefficients were obtained by means of the Raman lidar method. A distance of 300 m to the mean cloud layer base was usually sufficient to avoid that particle water-uptake effects influenced $\alpha_p$. Water uptake occurs when the relative humidity increases from values below about 60 % towards 100 % at cloud base (see examples in Schmidt et al., 2014a). As cloud properties we selected CDNC and droplet effective radius for distinct layers from 0–30 m, 30–70 m, and 70–120 m above cloud base.





ACPD
14, 31409–31440, 2014



Figure 2 shows a first overview of our lidar-based ACI studies. For 26 cloud cases the correlation between cloud droplet effective radius in the 30–70 m cloud layer (30–70 m above cloud base) and aerosol particle extinction coefficient $\alpha_p$ below cloud base is shown. Vertical wind information is not taken into account in this figure, i.e., the presented findings are based on lidar signal averages without any sorting of signals to updraft or downdraft periods. Typical signal averaging periods ranged from 10–90 min.

As can be seen, the computed $ACI_r$ values for two groups of LWC ranges are small. The $ACI_r$ values are $0.10 \pm 0.17$ and $-0.01 \pm 0.09$ for the lower and higher LWCs cloud groups, respectively. The overall mean value of $ACI_r$ value is $0.04 \pm 0.09$. The coefficients of determination $R^2$ from the linear regression of the $ACI_r$ calculation are 0.03 and $< 0.01$ for the data set with the lower and higher LWC, respectively.

Figure 3 shows the correlation between CDNC and $\alpha_p$ for the 26 dual-FOV Raman lidar measurements. On average, higher CDNCs are found for larger particle extinction coefficients. This tendency is expressed in an $ACI_N$ value of $0.32 \pm 0.19$. The coefficient of determination obtained from the linear regression for the calculation of $ACI_N$ is low with 0.10. Again, upward and downward motions were not taken into account in the data analysis.

The large scatter in the observational data reflects the impact of atmospheric variability (varying meteorological conditions), uncertainties in the retrieved cloud properties (50–100 % relative error), and also that the particle extinction coefficient $\alpha_p$ is not the optimum aerosol proxy. The CCN concentration (aerosol particles with radii of roughly 50 nm and larger) would be the optimum aerosol parameter. Based on our long-term Aerosol Robotic Network (AERONET) photometer measurements of column-integrated aerosol optical thickness (AOT at 500 nm) and corresponding particle size distribution at Leipzig we observed that the CCN concentration can vary within an order of magnitude for a given extinction coefficient.





ACPD
14, 31409–31440, 2014



### 3.3 $ACI_N$: damping effect by mixing and entrainment

Figure 4 presents the cloud-aerosol data sets with cloud properties measured within the cloud layer from cloud base to 30 m above cloud base and for the layer from 70–120 m above cloud base. Together with Fig. 3 (cloud layer from 30–70 m above cloud base) the results show the decreasing strength of the observed aerosol-cloud interaction with height above cloud base. Schmidt et al. (2013) stated that lidar observations at cloud base have to be exercised with caution because small variations in the cloud base height may lead to an inclusion of cloud free air in the cloud retrievals and may introduce a bias. Disregarding this potential bias, the aerosol-cloud interaction effect is smallest in the cloud layer from 70–120 m with $ACI_N = 0$ and strongest just above cloud base ($ACI_N = 0.38$). Turbulent vertical mixing and entrainment of cloud-free and drier air from above probably weakened the aerosol effect on CDNC in the upper part of the shallow cloud layers. Entrainment of dry air may lead to a strong reduction of CDNC (evaporation of small droplets) and may significantly change the cloud droplet size distribution by collison and coagulation of droplets of different sizes in the upper cloud parts, and thus the droplet effective radii as discussed by Kim et al. (2008).

The dependence of $ACI_N$ on height above cloud base (laser penetration depth) as shown in Figs. 3 and 4 is summarized in Fig. 5 (green bars). The corresponding coefficients of determination for $ACI_N$ are compared in Fig. 6 to corroborate the statistical significance of our findings. The coefficients of determination show a strong decrease from the penetration depth of 30–70 m to 70–120 m.

### 3.4 $ACI_N$ during updraft periods

The main goal of Fig. 5, however, is to demonstrate the necessity to include vertical-wind information in ACI studies in layered clouds over a continental site. We contrast the results discussed before with our findings when vertical wind information, i.e., the knowledge on the occurrence of updrafts, is explicitly taken into account in the lidar signal averaging procedures. In the case of the red bars in Fig. 5, the basic lidar signal





ACPD
14, 31409–31440, 2014



average profiles exclusively consider lidar returns measured during periods with positive vertical wind component. Several examples showing the strong influence of the vertical air motion on cloud properties and aerosol-cloud interactions were discussed in Schmidt et al. (2014a). Unfortunately, the number of co-located dual-FOV and Doppler lidar observations is about 50 % lower than the number of measured cloud cases with dual-FOV lidar alone. 13 cases of combined dual-FOV Raman lidar and Doppler wind lidar observations could finally be used for the calculation of the ACI values in Fig. 5 (red bars).

As can be seen, $ACI_N$ is strongly increased for the updraft periods. Obviously a well-defined flow of CCN into clouds occurs during the updraft periods. A large decrease of $ACI_N$ is found again with increasing cloud penetration depth from 30–70 m to 70–120 m. This cloud penetration-depth effect may be especially large in our case of free-tropospheric cloud layers (over land) which develop at comparably stable environmental conditions.

In the cloud layer from 30–70 m above cloud base, the $ACI_N$ value for updraft regions is $0.78 \pm 0.36$ and thus a factor of two larger than the corresponding $ACI_N$ value derived without consideration of the vertical wind velocity. The good correlation between the aerosol proxy and CDNC during updraft periods is corroborated by Fig. 6. The corresponding coefficient of determination reaches almost a value of 0.3 which is about a factor of three larger than the value derived without consideration of the vertical wind velocity.

For the updraft periods, $ACI_N$ is lower in the lowest 30 m above cloud base compared to the values for the 30–70 m cloud layer. Furthermore, the corresponding coefficient of determination is lower for the lowest 30 m of the cloud than for the 30–70 m layer. Obviously, the results in the lowest 30 m of the clouds are affected by retrieval inaccuracies due to variations of the cloud base height (during the updraft periods) as discussed above. From the trend that $ACI_N$ decreases with increasing cloud penetration depth (within the 30–120 m height range) we may conclude that $ACI_N$ is close to 1.0 at cloud base during updraft periods. In agreement with Kim et al. (2008), we may also con-





ACPD
14, 31409–31440, 2014



clude from our studies that downdrafts, turbulent mixing, and entrainment processes immediately begin to reduce any clear aerosol effect on cloud microphysical properties on the way up through the cloud layer.

## 4 Literature review

We checked the literature concerning field studies of aerosol-cloud interactions of warm clouds of the past two decades for available ACI numbers. Main motivation was to answer the question how well our results are in agreement with other findings and what are the consequences in the ACI studies when vertical wind information is not available or not taken into account. Figure 7 summarizes this survey and may be regarded as an update of former efforts of ACI compilations (Twohy et al., 2005; Lu et al., 2008; McComiskey and Feingold, 2008, 2012). In the majority of considered satellite observations (red bars in Fig. 7) and airborne measurements (blue bars in Fig. 7), maritime layered clouds were investigated. With few exceptions, vertical wind information was not available or not considered. As can be seen, almost the full range of physically meaningful $ACI_N$ values from 0 (no aerosol influence) to 1 (linear increase of CDNC with aerosol burden) is covered by observations. Even values > 1 are reported.

### 4.1 $ACI_N$ from satellite remote sensing

The wide spread of derived ACI values reflects first of all the use of different platforms (ground-based, airborne, spaceborne) and methods (different combinations of in situ measurements, active remote sensing, and passive remote sensing). As discussed in detail by McComiskey and Feingold (2012), the main reason for the relatively low $ACI_N$ values obtained from satellite passive remote sensing is that the analysis scale is in strong disagreement with the process scale. Aerosols influence cloud properties at the microphysical scale (process scale), but observations are most made of bulk properties over a wide range of resolutions (analysis scales). The most accurate representation





ACPD
14, 31409–31440, 2014



of a process results from an analysis in which the process scale and analysis scale are the same. Typical cloud scales of variability (process scales, 100–1000 m) are much smaller than the scales of variability in the aerosol properties (10–100 km). Considering scales that drive convection, spatial scales of 10 to 100 m adequately capture bulk cloud properties. These small scales of variability may be observable from in situ and ground-based measurements but typically not from space, McComiskey and Feingold (2012) concluded.

Furthermore, radiation scattered by cloud edges can brighten the aerosol fields around clouds and can in this way systematically disturb the retrieval of aerosol optical depth and cloud properties used in satellite-based passive remote sensing ACI studies. Particle water-uptake in the aerosol layers around the clouds and lofted aerosol layers above the clouds (Painemal et al., 2014) are further sources of errors in the ACI studies from space. Aerosols detected and quantified around the cloud fields may not represent the desired aerosol conditions below cloud base.

Ma et al. (2014) recently reassessed the satellite data analysis presented in Quaas et al. (2008) (both papers are considered in Fig. 7) and included a longer time period. As a global average for cloud fields over the oceans, they found an $ACI_N$ value close to 0.4 from their state-of-the-art satellite observations. The study of Ma et al. (2014) offers the opportunity to discuss differences between ACI studies over continents (as our study) and oceans (most studies in Fig. 7). In contrast to the global mean $ACI_N$ value close to 0.4 over the oceans, they derived a global average $ACI_N$ value in the range of 0.1–0.15 over the continents (not shown in Fig. 7). The reason for the strong contrast between the $ACI_N$ values for clouds over land and sea may be related to the fact that the observed cloud fields over oceans form at comparably simple meteorological and aerosol conditions. The studied short-lived cumuli fields or aged stratocumulus layers mostly develop within a well-mixed, undisturbed marine boundary layer at almost adiabatic-like stratification of the water content resulting in an height-independent CDNC from cloud base to top (Painemal and Zuidema, 2013). Effects of vertical motions (updrafts, turbulent mixing, and entrainment of drier air into the clouds) were found





ACPD
14, 31409–31440, 2014



to have a comparably low impact on airborne ACI studies over maritime sites (Twohy et al., 2005; Terai et al., 2012; Werner et al., 2014).

In contrast, over land much more complex aerosol conditions (layering, spatial and temporal variability, composition, size distributions, mixtures of different aerosol types) prevail. Furthermore, the daily development of the boundary layer and nocturnal evolution of the residual layer lead to permanent changes in the updraft/downdraft characteristics (strengths, spatial distribution) in the lower troposphere up to several kilometers height. Orographic effects continuously disturb the air flow and may trigger gravity waves (and thus vertical motions) which influence cloud formation and microphysical properties in a complicated way. Over continents, vertical motions play a much stronger role in cloud processes and thus presumably lead to a much stronger bias in the ACI characterization if not considered.

Case A in Fig. 7 (orange bar A) supports this hypothesis. In our simplified approach we assumed a CDNC profile up to 120 m above cloud base as derived from the dual-FOV Raman lidar observations and that CDNC is height-independent (and equal to the value at 120 m) for the rest of the cloud up to cloud top. The corresponding vertically integrated cloud values of CDNC were then combined with the lidar-derived aerosol particle extinction coefficients to determine the $ACI_N$ value. Case A may oversimplify the usually complex cloud features over polluted continental sites, but the low $ACI_N$ value of 0.11 points to the right direction and is rather close to the global mean value obtained by Ma et al. (2014) of 0.1–0.15 over the continents. By means of satellite remote sensing the impact of vertical motions (strengthening of ACI during updraft periods, diminishing during downdraft periods) can not be resolved so that a strong underestimation of ACI is not surprizing.

### 4.2 $ACI_N$ from airborne observations

In strong contrast to the findings from spaceborne remote sensing, the majority of airborne observations lead to $ACI_N$ values of mostly > 0.6, as can be seen in Fig. 7. Most of these studies deal with shallow marine boundary-layer clouds (stratocumulus





ACPD
14, 31409–31440, 2014



fields, convective cumuli), are based on directly (in situ) measured aerosol particle number concentrations below cloud base, and consider the accumulation mode particle fraction only, i.e., particles with diameters larger than 80–100 nm, which best represent the CCN fraction. Cloud microphysical information from cloud base to top was used in most ACI analyses. Most studies did not consider vertical motion.

However, several attempts are available in which the sensitivity of the ACI values on vertical motion was illuminated. McComiskey et al. (2009) investigated coastal stratiform clouds in California and found an increase of the mean $ACI_N$ value from 0.48 to 0.58 (for updraft periods with vertical winds $> 0.5\,m\,s^{-1}$) and 0.69 (for periods with vertical winds $> 1\,m\,s^{-1}$). McFarquhar and Heymsfield (2001) investigated aerosol-cloud relationships over the Indian Ocean and found only a slight increase in the mean $ACI_N$ values from 0.63, to 0.67 and 0.7 for data sets, considering only data for which the vertical winds were < 0.5, from > 0.5–2, and $> 2\,m\,s^{-1}$ in tropical cloud layers, respectively. Werner et al. (2014) found that updraft velocity variations from 0.5 to $4\,m\,s^{-1}$ caused variations in the derived $ACI_r$ values by 0.02, or in terms of $ACI_N$ by 0.06. They concluded that updraft velocity strength is of minor importance in aerosol-cloud interaction studies of short-lived tropical trade wind cumuli over the tropical Atlantic. However, it is also interesting to note that Lu et al. (2008) found that better regression between maritime cloud and aerosol parameters is obtained when CDNC, accumulation mode particle number concentration $N_{acc}$, and vertical velocity is considered in the regression study. The CDNC/$N_{acc}$ ratio increased by about 30 % for updraft speeds around $2\,m\,s^{-1}$ compared to the CDNC/$N_{acc}$ ratio for a vertical velocity of $0.5\,m\,s^{-1}$.

An interesting approach (leading to a high study-mean ACI of 0.86) is presented by Painemal and Zuidema (2013). They combined airborne fast (1 Hz sampling) in situ measurements of $N_{acc}$ below the cloud with cloud optical depth and liquid water path values obtained from simultaneous observations (also at 1 Hz resolution) with upward-looking broadband irradiance and narrow field-of-view millimeter-wave radiometers. The authors argued that this approach works well over the oceans (in the boundary layer) when the cloud structure is well described by adiabatic conditions and corre-





ACPD
14, 31409–31440, 2014



sponding height-independent CDNC profile, but may not work over continents with the mentioned complex cloud processes and aerosol conditions.

The maximum values of $ACI_N$ close to 1.05 in Fig. 7 are obtained from helicopter-borne observations of tropical, short-lived trade-wind cumuli around Barbados (Werner et al., 2014; Ditas, 2014). Werner et al. (2014) used two stacked payloads which were attached on top of each other to a helicopter by means of a 160 m long rope to perform in situ measurements within and collocated radiation measurements above clouds, 140 m above the in-situ aerosol and cloud observational platform which was attached to the end of the rope. The helicopter was moving with a comparably low horizontal speed of 15–20 $m\,s^{-1}$. The observed clouds had horizontal extensions from 300–3000 m. The aerosol information for the ACI studies was taken from measurements in the subcloud layer (from the surface up to 400 m height). As aerosol proxy they used the aerosol particles number concentrations considering particles with diameter > 80 nm only. Daily mean cloud effective radii (from the radiation measurements above the cloud) were combined with daily mean aerosol concentrations, measured in November 2010 and April 2011. Werner et al. (2014) found high $ACI_r$ around 0.35 (i.e., $ACI_N$ around 1.05) from these aerosol and cloud observations.

Ditas (2014) used the same cloud cases, but an alternative approach to study ACI. Only updraft periods were used in these ACI studies. The aerosol particle concentration outside of clouds was compared with the aerosol particle number concentrations inside the cloud layer. The difference between the two aerosol number concentrations was then interpreted as the activated particle number concentration (and taken as a proxy for CDNC) in the ACI studies. This approach is corroborated by a study of Zheng et al. (2011) in which a clear and strong dependence between measured CCN (for a relative humidity of 100.2 %) and CDNC was observed over the Pacific west of Chile.

### 4.3 $ACI_N$ from ground-based observations

Figure 7 also includes $ACI_N$ values (from 0.25 to 0.5) obtained from ground-based observations (green bars in Fig. 7) when combining aerosol data measured at the surface





ACPD
14, 31409–31440, 2014



or at low heights with mostly column-integrated cloud properties which were retrieved from radiometer observations or from combined cloud radar and radiometer observations. These studies include clouds (convective and stratiform clouds) developing over land. The combination of surface aerosol information and remotely sensed cloud properties (mean values from base to top) is obviously only a rough approach (at least over land) to identify an impact of given aerosol conditions on cloud evolution and resulting properties for the reasons discussed above. Furthermore, $ACI_N$ values in Fig. 7 reported by Feingold et al. (2003) and McComiskey et al. (2009) are based on total aerosol particle number concentration, which include size ranges that are below the activation diameter for cloud droplets (Werner et al., 2014). This fact also reduces the calculated ACI values.

Finally, we include our own observations (case B in Fig. 7). Case B is simply taken from Fig. 5 (red bar for the 30–70 m layer) and considers the detailed information on particle extinction below cloud base, CDNC just above cloud base, and updraft periods in the data analysis. As mentioned, we concluded from our studies that $ACI_N$ probably approaches values around at 1.0 at cloud base during updraft periods.

### 4.4 Literatur review: conclusions

In summary, we may conclude from Fig. 7 that all CCN become activated at cloud base when injected into the cloud from below, and correspondingly that $ACI_N$ is close to 1.0 at cloud base, disregarding whether the clouds are over the ocean or over continents. We can further conclude that the consideration of vertical motions in the ACI studies may not be relevant in cases of cloud layers which develop in the boundary layer over the oceans, but must be kept in consideration in aerosol-cloud studies over continents. Finally, we can conclude that observations (and data analysis methods) yielding $ACI_N$ numbers far below 1, i.e. $< 0.5$, must at least be interpreted with care. In agreement with the extended discussion in the literature, it is obvious that satellite observations, focusing on ACI (with values mainly below 0.4), may not be appropriate to guide climate modelling activities (Quaas et al., 2009; Ban-Weiss et al., 2014; Ma et al., 2014).





ACPD
14, 31409–31440, 2014



## 5 Conclusions

Twenty nine cases of liquid-water cloud systems were observed with a novel dual-FOV Raman lidar over the polluted central European site of Leipzig, Germany, between September 2010 and September 2012. A collocated Doppler lidar was employed to provide measurements of up and downward motions at cloud base. The key results of the statistical analysis were presented and showed a clear aerosol signature on cloud evolution and CDNC in the lowest part of convectively weak cloud layers during updraft periods with $ACI_N$ approaching most probably 1.0 at cloud base. A strong impact of meteorological effects (turbulent mixing, entrainment of dry air) towards a weakening of the aerosol effect at heights higher up in the cloud layer was also revealed in the stratiform cloud layers.

The comparison of the retrieved $ACI_N$ values showed good agreement with published aircraft observations of ACI, but also that passive satellite remote sensing delivers much lower $ACI_N$ values in comparison to our lidar and the airborne observations. Satellite-derived values of the indirect aerosol effect (warm clouds, albedo effect) may not provide a representative picture of the true impact of aerosols on the microphysical properties of liquid clouds.

Because of the complex and combined influences of meteorological and aerosol-related processes on cloud evolution and lifetime, especially of vertical motions, strong efforts regarding field observations (in networks, in the framework of extended field campaigns) of aerosol and cloud properties and vertical velocity are requested especially over the continents, covering all cloud types (convective and stratiform cloud systems) from the tropics to the poles, in order to improve our knowledge on the impact of man-made aerosols on cloud formation in the atmospheric system. In the second step, climate models equipped with sophisticated cloud-process-resolving modules must be able to reproduce these observations, especially the injection of aerosol particles into the lowest part of the cloud layer and the consequences in the evolution of the cloud layer. All meteorological and aerosol aspects must be properly simulated. In the third





ACPD
14, 31409–31440, 2014



step, the so-called cloud albedo effect (Twomey, 1974, 1977) may then be computed. But one should keep in mind that this effect is just one of numerous aerosol effects on climate.

*Acknowledgements.* The presented work was facilitated by the support of the whole group for ground-based remote sensing of the TROPOS institute. Fruitful discussions with Florian Ditas contributed to the work. The research leading to these results has received funding from the European Union Seventh Framework Programme (FP7/2007-2013) under grant agreement n 262254 (Aerosols, Clouds, and Trace gases Research Infrastructure Network, ACTRIS).

## References

Ansmann, A., Tesche, M., Seifert, P., Althausen, D., Engelmann, R., Fruntke, J., Wandinger, U., Mattis, I., and Müller, D.: Evolution of the ice phase in tropical altocumulus: SAMUM lidar observations over Cape Verde, J. Geophys. Res., 114, D17208, doi:10.1029/2008JD011659, 2009. 31413

Ansmann, A., Fruntke, J., and Engelmann, R.: Updraft and downdraft characterization with Doppler lidar: cloud-free versus cumuli-topped mixed layer, Atmos. Chem. Phys., 10, 7845–7858, doi:10.5194/acp-10-7845-2010, 2010. 31413

Ban-Weiss, G. A., Jin, L., Bauer, S. E., Bennartz, R., Liu, X., Zhang, K., Ming, Y., Guo, H., and Jiang, J. H.: Evaluating clouds, aerosols, and their interactions in three global climate models using satellite simulators and observations, J. Geophys. Res.-Atmos., 119, 10876–10901, doi:10.1002/2014JD021722, 2014. 31424

Bréon, F., Tanré, D., and Generoso, S.: Aerosol effect on cloud droplet size monitored from satellite, Science, 295, 834–838, doi:10.1126/science.1066434, 2002.

Bühl, J., Ansmann, A., Seifert, P., Baars, H., and Engelmann, R.: Toward a quantitative characterization of heterogeneous ice formation with lidar/radar: comparison of CALIPSO/CloudSat with ground-based observations, Geophys. Res. Lett., 40, 4404–4408, doi:10.1002/grl.50792, 2013. 31413

Bulgin, C. E., Palmer, P. I., Thomas, G. E., Arnold, C. P. G., Campmany, E., Carboni, E., Grainger, R. G., Poulsen, C., Siddans, R., and Lawrence, B. N.: Regional and seasonal variations of the Twomey indirect effect as observed by the ATSR-2 satellite instrument, Geophys. Res. Lett., 35, L02811, doi:10.1029/2007GL031394, 2008.





ACPD
14, 31409–31440, 2014



Costantino, L. and Bréon, F.-M.: Aerosol indirect effect on warm clouds over South-East Atlantic, from co-located MODIS and CALIPSO observations, Atmos. Chem. Phys., 13, 69–88, doi:10.5194/acp-13-69-2013, 2013.

Ditas, F.: Microphysical properties of aerosol particles in the trade wind regime and their influence on the number concentration of activated particles in trade wind cumulus clouds, Ph.D. thesis, University of Leipzig, Leipzig, 2014. 31423

Engelmann, R., Wandinger, U., Ansmann, A., Müller, D., Zeromskis, E., Althausen, D., and Wehner, B.: Lidar observations of the vertical aerosol flux in the planetary boundary layer, J. Atmos. Ocean. Tech., 25, 1296–1306, 2008. 31413

Feingold, G., Remer, L., Ramaprasad, J., and Kaufman, Y.: Analysis of smoke impact on clouds in Brazilian biomass burning regions: an extension of Twomey's approach, J. Geophys. Res., 106, 22907–22922, doi:10.1029/2001JD000732, 2001. 31414

Feingold, G., Eberhard, W. L., Veron, D. E., and Previdi, M.: First measurements of the Twomey indirect effect using ground-based remote sensors, Geophys. Res. Lett., 30, 1287, doi:10.1029/2002GL016633, 2003. 31424

Garrett, T. J., Zhao, C., Dong, X., Mace, G. G., and Hobbs, P. V.: Effects of varying aerosol regimes on low-level Arctic stratus, Geophys. Res. Lett., 31, L17105, doi:10.1029/2004GL019928, 2004. 31414

Ghan, S. J., Chuang, C. C., and Penner, J. E.: A parameterization of cloud droplet nucelation, I, single aerosol type, Atmos. Res., 30, 197–211, 1993. 31411

Ghan, S. J., Leung, L. R., Easter, R. C., and Abdul-Razzak, H.: Prediction of cloud droplet number in a general circulation model, J. Geophys. Res., 102, 21777–21794, doi:10.1029/97JD01810, 1997. 31411

Ghan, S. J., Abdul-Razzak, H., Nenes, A., Ming, Y., Liu, X., Ovchinnikov, M., Shipway, B., Meskhidze, N., Xu, J., and Shi, X.: Droplet nucleation: physically-based parameterizations and comparative evaluation, J. Adv. Model. Earth Syst., 3, M10001, doi:10.1029/2011MS000074, 2011. 31411

Gultepe, I., Isaac, G., Leaitch, W., and Banic, C.: Parameterizations of marine stratus microphysics based on in situ observations: implications for GCMs, J. Climate, 9, 345–357, doi:10.1175/1520-0442(1996)009<0345:POMSMB>2.0.CO;2, 1996.

Illingworth, A. J., Hogan, R. J., O'Connor, E. J., Bouniol, D., Delanoe, J., Pelon, J., Protat, A., Brooks, M. E., Gaussiat, N., Wilson, D. R., Donovan, D. P., Klein Baltink, H., van Zadelhoff, G.-J., Eastment, J. D., Goddard, J. W. F., Wrench, C. L., Haeffelin, M., Krasnov, O. A., Russchen-





ACPD
14, 31409–31440, 2014



berg, H. W. J., Piriou, J.-M., Vinit, F., Seifert, A., Tompkins, A. M., and Willen. J., CLOUDNET: continuos evaluation of cloud profiles in seven operational models using ground-based observations, B. Am. Meteorol. Soc., 88, 883–898, 2007. 31411

Kim, B.-G., Schwartz, S. E., and Miller, M. A.: Effective radius of cloud droplets by ground-based remote sensing: relationship to aerosol, J. Geophys. Res., 108, D23, doi:10.1029/2003JD003721, 2003.

Kim, B.-G., Miller, M. A., Schwartz, S. E., Liu, Y., and Min, Q.: The role of adiabaticity in the aerosol first indirect effect, J. Geophys. Res., 113, D05210, doi:10.1029/2007JD008961, 2008. 31417, 31418

Lu, M.-L., Conant, W. C., Jonsson, H. H., Varutbangkul, V., Flagan, R. C., and Seinfeld, J. H.: The marine stratus/stratocumulus experiment (MASE): aerosol-cloud relationship in marine stratocumulus, J. Geophys. Res., 112, D10209, doi:10.1029/2006JD007985, 2007.

Lu, M.-L., Feingold, G., Jonsson, H. H., Chuang, P. Y., Gates, H., Flagan, R. C., and Seinfeld, J. H.: Aerosol-cloud relationships in continental shallow cumulus, J. Geophys. Res., 113, D15201, doi:10.1029/2007JD009354, 2008. 31419, 31422

Ma, X., Yu, F., and Quaas, J.: Reassessment of satellite-based estimate of aerosol climate forcing, J. Geophys. Res. Atmos., 119, 10394–10409, doi:10.1002/2014JD021670, 2014. 31420, 31421, 31424

Martin, G. M., Johnson, D. W., and Spice, A.: The measurement and parameterization of effective radius of droplets in warm stratocumulus clouds, J. Atmos. Sci., 51, 1823–1842, doi:10.1175/1520-0469(1994)051<1823:TMAPOE>2.0.CO;2, 1994.

Mattis, I., Ansmann, A., Müller, D., Wandinger, U., and Althausen, D.: Multiyear aerosol observations with dual-wavelength Raman lidar in the framework of EARLINET, J. Geophys. Res., 109, D13203, doi:10.1029/2004JD004600, 2004. 31415

McComiskey, A. and Feingold, G.: Quantifying error in the radiative forcing of the first aerosol indirect effect, Geophys. Res. Lett., 35, L02810, doi:10.1029/2007GL032667, 2008. 31414, 31419

McComiskey, A. and Feingold, G.: The scale problem in quantifying aerosol indirect effects, Atmos. Chem. Phys., 12, 1031–1049, doi:10.5194/acp-12-1031-2012, 2012. 31419, 31420

McComiskey, A., Feingold, G., Frisch, A. S., Turner, D. D., Miller, M. A., Chiu, J. C., Min, Q., and Ogren, J. A.: An assessment of aerosol-cloud interactions in marine stratus clouds based on surface remote sensing, J. Geophys. Res., 114, D09203, doi:10.1029/2008JD011006, 2009. 31414, 31422, 31424





ACPD
14, 31409–31440, 2014



Morales, R. and Nenes, A.: Characteristic updrafts for computing distribution-averaged cloud droplet number and stratocumulus cloud properties, J. Geophys. Res., 115, D18220, doi:10.1029/2009JD013233, 2010. 31411

McFarquhar, G. and Heymsfield, A.: Parameterizations of INDOEX microphysical measurements and calculations of cloud susceptibility: applications for climate studies, J. Geophys. Res., 106, 28675–28698, doi:10.1029/2000JD900777, 2001. 31422

Nakajima, T., Higurashi, A., Kawamoto, K., and Penner, J.: A possible correlation between satellite-derived cloud and aerosol microphysical parameters, Geophys. Res. Lett., 28, 1171–1174, doi:10.1029/2000GL012186, 2001.

O'Dowd, C., Lowe, J., Smith, M., and Kaye, A.: The relative importance of non-sea-salt sulphate and sea-salt aerosol to the marine cloud condensation nuclei population: an improved multi-component aerosol-cloud droplet parametrization, Q. J. Roy. Meteor. Soc., 125, 1295–1313, doi:10.1002/qj.1999.49712555610, 1999.

Painemal, D. and Zuidema, P.: The first aerosol indirect effect quantified through airborne remote sensing during VOCALS-REx, Atmos. Chem. Phys., 13, 917–931, doi:10.5194/acp-13-917-2013, 2013. 31420, 31422

Painemal, D., Kato, S., and Minnis, P.: Boundary layer regulation in the southeast Atlantic cloud microphysics during the biomass burning season as seen by the A-train satellite constellation, J. Geophys. Res.-Atmos., 119, 11288–11302, doi:10.1002/2014JD022182, 2014. 31420

Quaas, J., Boucher, O., and Breon, F.: Aerosol indirect effects in POLDER satellite data and the Laboratoire de Meteorologie Dynamique-Zoom (LMDZ) general circulation model, J. Geophys. Res., 109, D08205, doi:10.1029/2003JD004317, 2004.

Quaas, J., Boucher, O., and Lohmann, U.: Constraining the total aerosol indirect effect in the LMDZ and ECHAM4 GCMs using MODIS satellite data, Atmos. Chem. Phys., 6, 947–955, doi:10.5194/acp-6-947-2006, 2006.

Quaas, J., Boucher, O., Bellouin, N., and Kinne, S.: Satellite-based estimate of the direct and indirect aerosol climate forcing, J. Geophys. Res., 113, D05204, doi:10.1029/2007JD008962, 2008. 31420

Quaas, J., Ming, Y., Menon, S., Takemura, T., Wang, M., Penner, J. E., Gettelman, A., Lohmann, U., Bellouin, N., Boucher, O., Sayer, A. M., Thomas, G. E., McComiskey, A., Feingold, G., Hoose, C., Kristjánsson, J. E., Liu, X., Balkanski, Y., Donner, L. J., Ginoux, P. A., Stier, P., Grandey, B., Feichter, J., Sednev, I., Bauer, S. E., Koch, D., Grainger, R. G.,





ACPD
14, 31409–31440, 2014



Kirkevåg, A., Iversen, T., Seland, Ø., Easter, R., Ghan, S. J., Rasch, P. J., Morrison, H., Lamarque, J.-F., Iacono, M. J., Kinne, S., and Schulz, M.: Aerosol indirect effects – general circulation model intercomparison and evaluation with satellite data, Atmos. Chem. Phys., 9, 8697–8717, doi:10.5194/acp-9-8697-2009, 2009. 31424

Raga, G. and Jonas, P.: On the link between cloud-top radiative properties and sub-cloud aerosol concentrations, Q. J. Roy. Meteor. Soc., 119, 1419–1425, doi:10.1002/qj.49711951410, 1993.

Ramanathan, V., Crutzen, P., Kiehl, J., and Rosenfeld, D.: Atmosphere – aerosols, climate, and the hydrological cycle, Science, 294, 2119–2124, doi:10.1126/Science.1064034, 2001.

Schmidt, J.: Dual-field-of-view Raman lidar measurments of cloud microphysical properties – investigation of aerosol-cloud intercations, Ph.D. thesis, University of Leipzig, Leipzig, 2014. 31411, 31413

Schmidt, J., Wandinger, U., and Malinka, A.: Dual-field-of-view Raman lidar measurments for the retrieval of cloud microphysical properties, Appl. Opt., 52, 2235–2247, 2013. 31411, 31413, 31417

Schmidt, J., Ansmann, A., Bühl, J., Baars, H., Wandinger, U., Müller, D., and Malinka, A. V.: Dual-FOV Raman and Doppler lidar studies of aerosol-cloud interactions: simultaneous profiling of aerosols, warm-cloud properties, and vertical wind, J. Geophys. Res., 119, 5512–5527, doi:10.1002/2013JD020424, 2014. 31412, 31413, 31414, 31415, 31418, 31435

Sekiguchi, M., Nakajima, T., Suzuki, K., Kawamoto, K., Higurashi, A., Rosenfeld, D., Sano, I., and Mukai, S.: A study of the direct and indirect effects of aerosols using global satellite data sets of aerosol and cloud parameters, J. Geophys. Res., 108, 4699, doi:10.1029/2002JD003359, 2003.

Terai, C. R., Wood, R., Leon, D. C., and Zuidema, P.: Does precipitation susceptibility vary with increasing cloud thickness in marine stratocumulus?, Atmos. Chem. Phys., 12, 4567–4583, doi:10.5194/acp-12-4567-2012, 2012. 31421

Twohy, C., Petters, M., Snider, J., Stevens, B., Tahnk, W., Wetzel, M., Russell, L., and Burnet, F.: Evaluation of the aerosol indirect effect in marine stratocumulus clouds: droplet number, size, liquid water path, and radiative impact, J. Geophys. Res., 110, D08203, doi:10.1029/2004JD005116, 2005. 31419, 31421

Twomey, S. A.: The nuclei of natural cloud formation. Part II: the supersaturation in natural clouds amd variation of cloud droplet concentration, Geofis. Pura Appl., 43, 243–249, 1959. 31411





ACPD
14, 31409–31440, 2014



Twomey, S.: Pollution and the planetary albedo, Atmos. Environ., 8, 1251–1256, 1974. 31426
Twomey, S.: Influence of pollution on shortwave albedo of clouds, J. Atmos. Sci., 34, 1149–1152, 1977. 31426
Wandinger, U., Seifert, P., Wagner, J., Engelmann, R., Bühl, J., Schmidt, J., Heese, B., Baars, H., Hiebsch, A., Kanitz, T., Althausen, D., and Ansmann, A.: Integrated remote-sensing techniques to study aerosols, clouds, and their interaction, in: Proceedings, 26th International Laser Radar Conference, Volume I, Porto Heli, Greece, 25–29 June 2012, 395–398, 2012. 31413
Werner, F., Ditas, F., Siebert, H., Simmel, M., Wehner, B., Pilewskie, P., Schmeissner, T., Shaw, R. A., Hartmann, S., Wex, H., Roberts, G. C., and Wendisch, M.: Twomey effect observed from collocated microphysical and remote sensing measurements over shallow cumulus, J. Geophys. Res.-Atmos., 119, 1534–1545, doi:10.1002/2013JD020131, 2014. 31421, 31422, 31423, 31424
Zheng, X., Albrecht, B., Jonsson, H. H., Khelif, D., Feingold, G., Minnis, P., Ayers, K., Chuang, P., Donaher, S., Rossiter, D., Ghate, V., Ruiz-Plancarte, J., and Sun-Mack, S.: Observations of the boundary layer, cloud, and aerosol variability in the southeast Pacific near-coastal marine stratocumulus during VOCALS-REx, Atmos. Chem. Phys., 11, 9943–9959, doi:10.5194/acp-11-9943-2011, 2011. 31423





ACPD
14, 31409–31440, 2014



**Table 1.** Aerosol and cloud properties of 29 studied aerosol-cloud scenarios. The range of observed aerosol extinction coefficients and cloud optical thicknesses and the corresponding mean values and standard deviations (SD) are given for 532 nm wavelength.

| | Range | Mean (±SD) |
|---|---|---|
| Aerosol extinct. coef. ($Mm^{-1}$) | 7–130 | 52 ± 34 |
| Cloud base height (m) | 1100–4400 | 2900 ± 910 |
| Cloud vertical extent (m) | 95–300 | 190 ± 50 |
| Cloud optical thickness | 1.5–5.9 | 3.6 ± 1.3 |
| LWP ($g\,m^2$) | 5.4–64 | 19 ± 4 |





ACPD
14, 31409–31440, 2014



**Table 2.** Statistics of cloud extinction coefficients (532 nm), droplet effective radii, LWCs, and CDNCs, derived from the dual-FOV Raman lidar observations. Range of values (minumum to maximum), mean values, and standard deviations (SD) are presented.

| | | Height range above cloud base | | |
|---|---|---|---|---|
| | | 0–30 m | 30–70 m | 70–120 m |
| Cloud extinction coefficient | Min ($km^{-1}$) | 2.6 | 3.9 | 5.1 |
| | Max ($km^{-1}$) | 28.3 | 36.3 | 44.4 |
| | Mean ($km^{-1}$) | 11.5 | 19.4 | 25.5 |
| | SD ($km^{-1}$) | 5.7 | 7.0 | 11.4 |
| Droplet effective radius | Min (µm) | 2.7 | 3.0 | 2.9 |
| | Max (µm) | 11.0 | 14.5 | 13.8 |
| | Mean (µm) | 5.8 | 9.0 | 10 |
| | SD (µm) | 1.9 | 3.0 | 2.6 |
| LWC | Min ($g\,m^{-3}$) | 0.010 | 0.012 | 0.020 |
| | Max ($g\,m^{-3}$) | 0.213 | 0.243 | 0.391 |
| | Mean ($g\,m^{-3}$) | 0.049 | 0.124 | 0.188 |
| | SD ($g\,m^{-3}$) | 0.041 | 0.063 | 0.102 |
| CDNC | Min ($cm^{-3}$) | 10 | 12 | 13 |
| | Max ($cm^{-3}$) | 460 | 545 | 496 |
| | Mean ($cm^{-3}$) | 112 | 92 | 72 |
| | SD ($cm^{-3}$) | 102 | 110 | 88 |





ACPD
14, 31409–31440, 2014



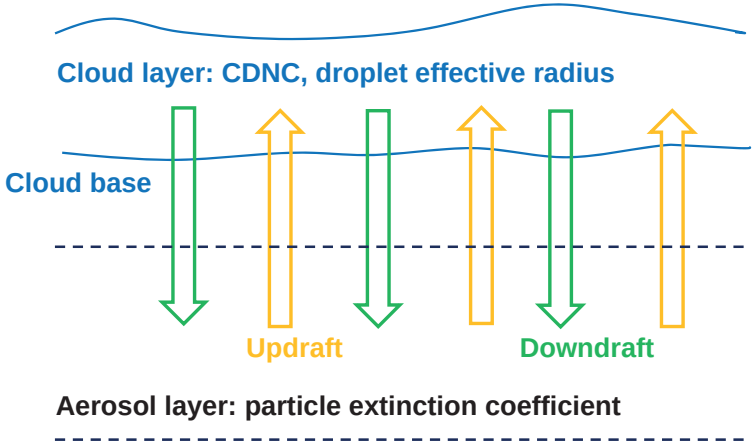


**Figure 1.** Sketch to illustrate our lidar-based approach to investigate aerosol-cloud interactions (ACI) in case of pure liquid-water clouds (blue lines indicate cloud bottom and top). The particle extinction coefficient measured with the Raman lidar in the height range from 300–1000 m below mean cloud base is used as aerosol proxy (dashed lines indicate base and top of the considered aerosol layer). From the dual-FOV Raman lidar observations we determine the cloud droplet number concentration (CDNC) and the effective radius for cloud layers from cloud base to 30 m above mean cloud base, from 30–70 m, and from 70–120 m above mean cloud base. A co-located Doppler lidar measures the vertical wind component and thus periods with updraft and downdraft motions.





ACPD
14, 31409–31440, 2014



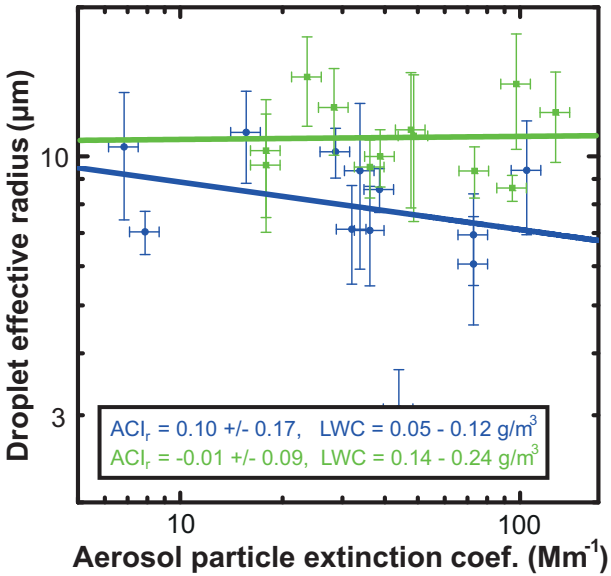


**Figure 2.** Cloud droplet effective radius (mean value for the height range from 30–70 m above cloud base) vs. aerosol particle extinction coefficient (mean value for the layer from 300–1000 m below cloud base). 26 cloud cases are considered. The corresponding $ACI_r$ values (negative slopes of the green and blue lines) are given as numbers together with the standard deviations. The overall mean $ACI_r$ value is $0.04 \pm 0.09$. Vertical wind information is not considered in this analysis. Error bars show the uncertainties in the retrieved aerosol and cloud parameters. An error discussion is given in Schmidt et al. (2014a).





ACPD
14, 31409–31440, 2014



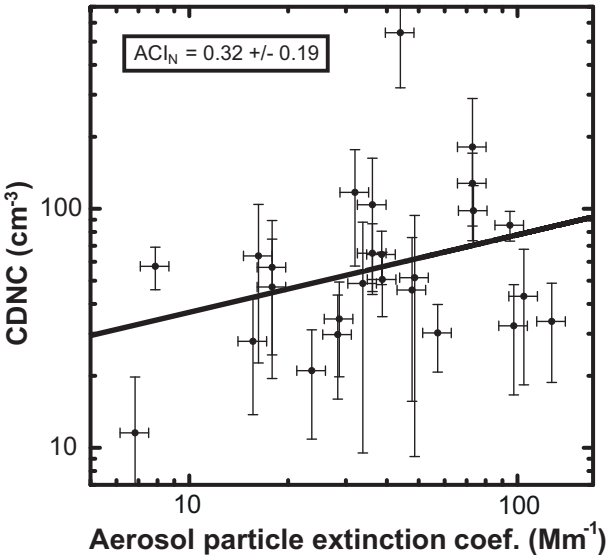


**Figure 3.** Cloud droplet number concentration (CDNC, for the 30–70 m layer above cloud base) vs. aerosol particle extinction coefficient (mean value for the layer from 300–1000 m below cloud base) for 26 dual-FOV Raman lidar probings. The linear regression of the data yields $ACI_N = 0.32 \pm 0.19$ (slope of the black line). Information of up- and downdraft periods is not considered in this analysis. Error bars show the retrieval uncertainties.





ACPD
14, 31409–31440, 2014



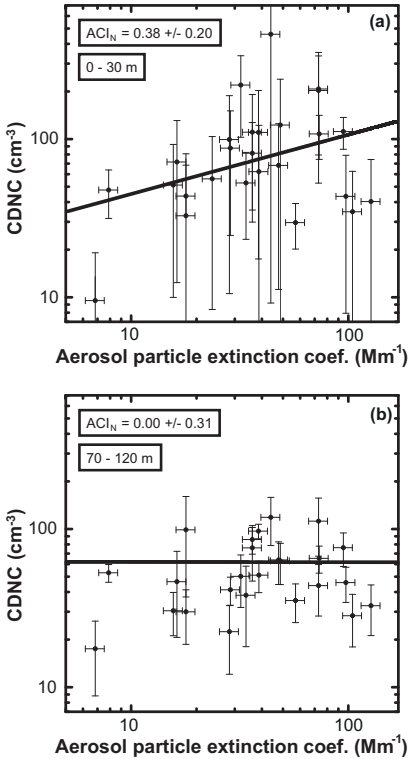


**Figure 4.** Same as Fig. 3, except for cloud layers from **(a)** cloud base to 30 m above cloud base and **(b)** for the 70–120 m layer above cloud base. The corresponding mean $ACI_N$ value and SD are given as numbers.





ACPD
14, 31409–31440, 2014



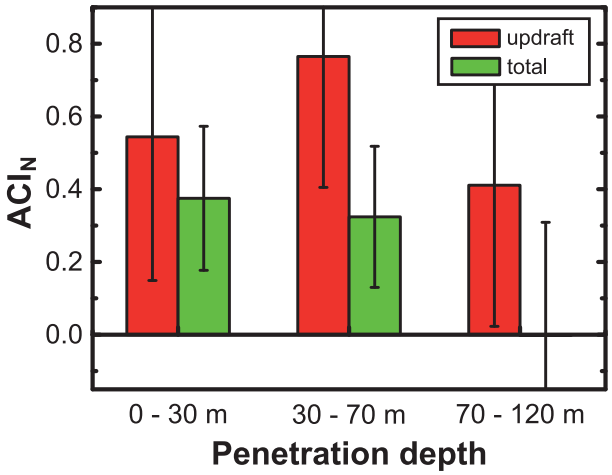


**Figure 5.** $ACI_N$ for updraft periods only (red, 13 cases) and when vertical wind information is not taken into account in the lidar data analysis and ACI retrieval (green, 26 cases). As aerosol proxy the layer mean particle extinction coefficient for the layer from 300 to 1000 m below cloud base is considered in the ACI retrieval. Penetration depth denotes height range above cloud base. Error bars show the overall variability caused by atmospheric variability and retrieval uncertainties.





ACPD
14, 31409–31440, 2014



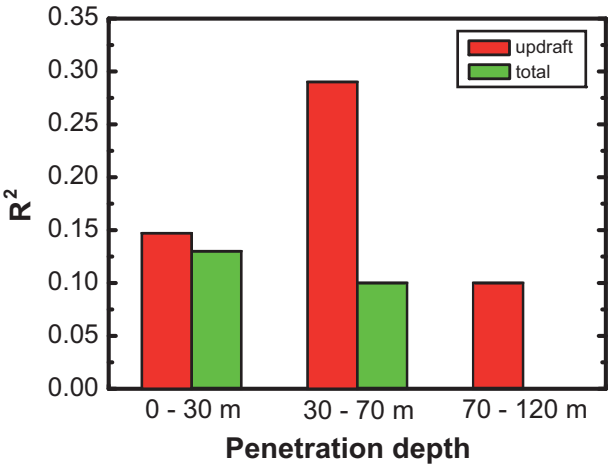


**Figure 6.** Coefficient of determination $R^2$ in the case of linear regression of aerosol proxy and CDNC to obtain $ACI_N$ as shown in Figs. 3 and 4. The green bars show $R^2$ when vertical wind information is ignored. The red bars are obtained when data only for updraft periods are considered in the linear regression.





ACPD
14, 31409–31440, 2014



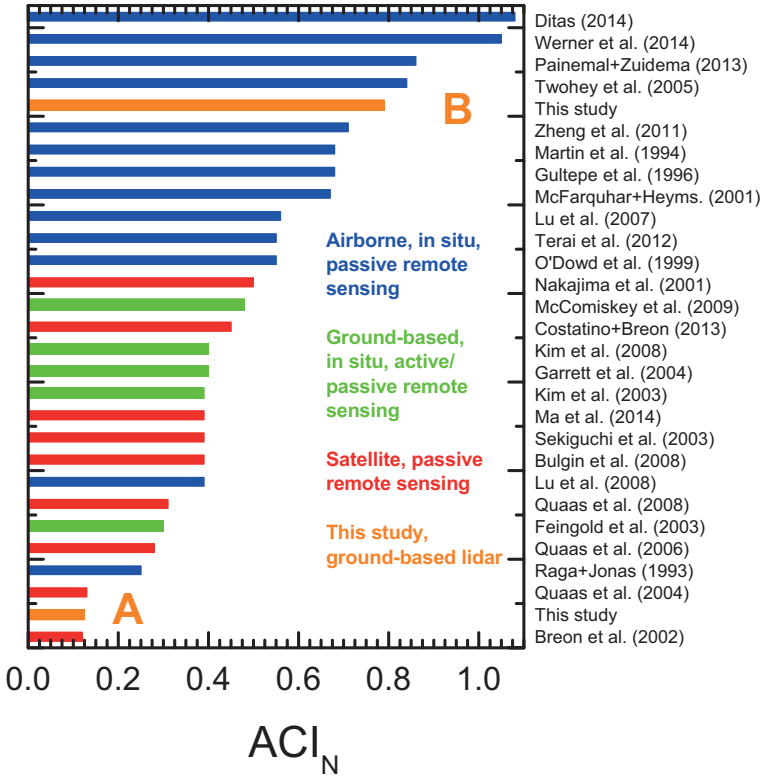


**Figure 7.** $ACI_N$ values as published in the literature (see references to the right). Different methods (in situ measurements, remote sensing) and observational platforms (aircraft, satellite, ground-based) are used. Case A (this study) makes use of the found aerosol and cloud properties (below the cloud, 0–30, 30–70, and 70–120 m layers above cloud base) for each cloud event and assumes that the cloud properties for the 70–120 m layer also hold for the rest of the cloud up to cloud top. Case B (this study) is from Fig. 5 (red bar, 30–70 m cloud penetration depth).





ACPD
14, 31409–31440, 2014